Integrated Retinal Amyloid Burden With Retinal Venular Tortuosity Predicts Verbal Memory Impairment

Oana Dumitrascu
Mayo Clinic Scottsdale: Mayo Clinic Arizona
Ryan Rosenberry
Cedars-Sinai Medical Center Department of Cardiology
Dale Sherman
Cedars-Sinai Medical Center
Maziyar M Khansari
University of Southern California Mark and Mary Stevens Neuroimaging and Informatics Institute
Julia Sheyn
Cedars-Sinai Medical Center Department of Neurosurgery
Tania Torbati
Cedars-Sinai Medical Center Department of Neurosurgery
Ayesha Sherzai
Loma Linda University
Dean Sherzai
Loma Linda University
Kenneth O. Johnson
NeuroVision Imaging, Inc.
Alan Czeszynski
NeuroVision Imaging, Inc.
Steven Verdooner
NeuroVision Imaging, Inc.
Keith L. Black
Cedars-Sinai Medical Center Department of Neurosurgery
Sally Frautschy
University of California Los Angeles
Patrick D. Lyden
Cedars-Sinai Department of Neurology
Yonggang Shi
University of Southern California Mark and Mary Stevens Neuroimaging and Informatics Institute
Zhaoyang Fan

BIRI: Cedars-Sinai Biomedical Imaging Research Institute
Susan Cheng
Cedars-Sinai Medical Center Department of Cardiology
Yosef Koronyo
Cedars-Sinai Medical Center Department of Neurosurgery
Maya Koronyo-Hamaoui (maya.koronyo@cshs.org)
Cedars-Sinai Medical Center https://orcid.org/0000-0003-2864-8442

Research

Keywords: retinopathy, retinal vessels, retinal fluorescence imaging, amyloid, cognitive decline, Alzheimer's disease

Posted Date: May 6th, 2021

DOI: https://doi.org/10.21203/rs.3.rs-481178/v1

Abstract

INTRODUCTION: Retinal imaging is a non-invasive tool to study retinal vasculature and neurodegeneration. Patients with mild cognitive impairment (MCI) and Alzheimer's disease (AD)-related cognitive disorder exhibit both retinal vascular abnormalities and intraretinal accumulation of amyloid beta-protein (Aβ) plaque. Curcumin-enhanced retinal fluorescence imaging (CRFI) was recently translated as a safe imaging tool for retinal Aβ plaque quantification, holding promise as an early-stage pathological biomarker of AD. In this exploratory study, we sought to determine whether retinal vascular features combined with retinal amyloid burden correlate with the neurocognitive status.

METHODS: We used scanning laser ophthalmoscopy to assess quantitative CRFI in a cohort of patients with cognitive impairment that underwent standard neuropsychological testing. Retinal blood vessels were segmented in a predefined circumpapillary region of interest. For each centerline, vessel tortuosity index, vessel inflection index and branching angle was quantified. Additionally, we automatically quantified retinal amyloid count in the supero-temporal quadrant and its subregions: posterior pole, proximal mid-periphery, and distal mid-periphery. Investigators performing quantifications were blinded to the subjects' clinical characteristics. Linear regression models were used to assess the correlations between retinal vascular and amyloid parameters and cognitive domain Z-scores.

RESULTS: In this pilot study, 34 subjects underwent automated retinal amyloid imaging and 29 subjects (55% female, mean age 64±6 years) had the combined retinal amyloid and peripapillary vascular analysis. Eleven subjects had normal cognition, 15 MCI, 2 probable AD and 1 non-AD dementia. CRFI was increased in individuals with impaired versus normal cognitive function (p 0.0012). Venous VTI was the most significant vascular parameter that differ across levels of CDR. Branching angle correlated with amyloid count in the distal mid-periphery (p=0.03), whereas vessel inflexion index correlated with posterior pole amyloid count (p=0.02). The combined proximal mid-periphery amyloid count – venous tortuosity index was found to exhibit highly significant group differences between cognitively impaired and cognitively normal subjects (0.49 ± 1.1 vs 0.91 ± 1.4, p=0.006). The combined proximal mid-periphery amyloid-venous tortuosity index also correlated with verbal memory (Wechsler Memory Scale-IV; p=0.001) and cognitive-related quality of life (SF-36 mental component score Z-scores; p=0.039).

CONCLUSION: Retinal venular tortuosity discriminates across cognitive scores and in combination with proximal mid-periphery amyloid count predicts verbal memory and cognitive-related quality-of-life. Future research is needed to confirm the clinical utility of this integrated retinal imaging-based methodology.

Background

By 2025, the number of people age 65 and older with Alzheimer's dementia (AD) is projected to reach 7.1 million — almost a 22% increase from 2020 (1, 2). The contribution of vascular disease to cognitive decline is increasingly recognized, as the mechanisms linking vascular dysfunction and neurodegeneration are better characterized (3–7). Recent reports implicate cerebral vascular pathology

as an early and core contributor to the development of AD (7–9), a chronic neurodegenerative condition and looming threat to public health (2, 10). The currently recognized pathological markers of AD, amyloid-beta (Aβ), tau, and neurodegeneration (11), are the central focus of multiple ongoing investigations for diagnostic biomarkers (12–15). Considering the emerging vascular hypothesis (8, 16–18), there is a critical need to incorporate vascular biomarkers into predictive models to allow for early and sensitive detection of burgeoning AD. Yet, imaging of the skull-shielded brain poses various limitations for widespread screening in the clinical setting. The retina is a central nervous system organ that exhibits many of the pathological hallmarks of AD (19–31) and is far more accessible for repeated and high-resolution imaging (32–40). Dysfunctional pericytes in the blood-brain barrier (BBB) are significant contributors to the pathogenesis of vascular cognitive impairment, including cerebral small vessel and large vessel disease and AD (26, 41). BBB pericyte injury is a predictor of apolipoprotein E (APOE) ε4–associated cognitive decline (4). Whereas the BBB mediates cerebral Aβ deposition, disruption of the retinal-blood barrier via retinopathy was shown to predict cognitive decline (26, 42–47). Post-mortem retinal vessels derived from patients with mild cognitive impairment (MCI) and AD exhibited early and progressive pericyte loss and Aβ accumulation inside retinal pericytes, correlating with similar AD pathology in the brain (26). Several studies demonstrated the linkage between cognitive deterioration and retinal vascular fractal dimensions, caliber, and tortuosity (43–49). Retinal arteriolar central reflex to vessel width ratio in digital retinal photographs was significantly higher in APOE ε4 allele carriers (46), hence the retina may allow for noninvasive monitoring of the effects of APOE ε4 on the cerebrovascular disease. Similarly, as targeting vascular risk factors is being considered in AD prevention trials (50), retinal vascular assessments could offer a window for assessing the response to various interventions.

Recent work has highlighted the promising utility of retinal fluorescence imaging, an emerging technique capable of non-invasively imaging and quantifying retinal amyloid, the pathological marker of AD (20, 21, 32). Using this technique, our group previously identified a significant association between retinal amyloid count, especially in the proximal mid-periphery, and the severity of cognitive impairment and hippocampal volume (32, 33). As the same retinal imaging modality also allows retinal vasculature analysis, we aimed to quantitatively examine both retinal vascular and retinal amyloid biomarkers in a cohort of subjects with cognitive decline. We sought to examine the relationship between retinal microvascular geometric features and retinal amyloid burden with global and domain-specific cognitive scores.

Methods

Participants

This study was approved by the Cedars-Sinai Institutional Review Board. All subjects older than 40 years of age, presenting to our Neurology clinic with subjective cognitive decline and interested in undergoing retinal fluorescence imaging were included in this cohort (Table 1). All subjects provided written informed consent prior to the commencement of the study.

Retinal Imaging

After ocular dilation, retinal imaging was performed with a confocal scanning ophthalmoscope (Retia^{TM}, CenterVue SpA) that utilizes blue light for excitation of curcumin emission to obtain fluorescent images of the retina, following a study design described in prior reports (Figure 1A) (32, 33). The investigators conducting the retinal image processing and quantifications were blinded to the patients' clinical characteristics.

Retinal amyloid quantification

Retinal images were processed using an automated retinal fluorescence measurement software system (NeuroVision Imaging, Inc.). A common region of interest (ROI) in the supero-temporal quadrant was applied with a field of view of 50 degrees positioned on the image center, using fovea and optic nerve head centers as reference points to correct for eye rotation, with a zone around the fovea and optic nerve head masked, as previously reported (33). The ROI was further divided into three subregions: posterior pole, proximal mid-periphery and distal mid-periphery (Figure 1B). Retinal amyloid count was quantified in the target ROI and the three specified subregions.

Retinal vascular quantification

From the same retinal fundus images, a ROI was defined within a circumpapillary region centered on optic nerve head (ONH) and extended between 1.5 and 4 ONH radii (51) (Figure 1C). Retinal vessels within the ROI were segmented using Frangi vesselness filter to generate a binary image (52). The vessels were classified into arteries and veins by a human observer based on the facts that retinal arteries are brighter in color and thinner in width compared to veins (53). For each vessel segment on the binary image, vessel endpoints were selected, and distance transformation was used to extract the vessel centerline. The extracted centerlines were smoothed using a cubic spline with a regularization parameter of 3 x 10-5. For each centerline, several geometric features including vessel tortuosity index (VTI), vessel inflection index, and branching angle were non-automatically quantified. VTI was calculated for each centerline based on combination of local and global centerline geometric variables as explained previously (54). Equation (1) shows formula for VTI,

$$(1)\ VTI = 0.1 \times (SD_{\theta}.N.M.^{L_A/L_C})$$

where is standard deviation of angle difference between lines tangent to each centerline pixel and a reference axis (i.e. x-axis). M is average ratio of centerline length to its chord length between pairs of inflection points including centerline endpoints. N is number of critical points where the first derivative of the centerline vanishes. LA and Lc are the length of the vessel and its chord length, respectively. VTI is shown to provide good correspondence with human perception of tortuosity and is invariant to rigid transformations. Similar to other measures of tortuosity, VTI is unitless. Its minimum value is zero while it has no theoretical maximum as it can increase with twistedness of a vessel. Vessel inflexion index was

determined based on number of inflection points along the vessels. Mathematically, these are pixels where the second derivative of centerline vanishes. Vessel inflexion index represents local changes in tortuosity of vessels and was found to be robust for ranking tortuosity of vessels with similar length (55). Branching angle of the vessels was calculated interactively using an open source tool GIMP 2.8.

Cognitive evaluation

All participants underwent a standard battery of neuropsychometric testing performed by a licensed neuropsychologist (DS). Standard neuropsychological testing included assessment of the Montreal Cognitive Assessment (MOCA), global Clinical Dementia Rating (CDR), general cognitive (ACS-Test of Premorbid Functioning) and specific cognitive domains: attention and concentration [Wechsler Adult Intelligence Scale (WAIS)-IV]; verbal memory [California Verbal Learning Test (CVLT) II, Wechsler Memory Scale (WMS)-IV Logical Memory II]; non-verbal memory [Rey Complex Figure Test and Recall (RCFT) 30 min, Brief Visuo-Spatial Memory Test Revised (BVMT-R) Delayed Recall]; language [Fluency-Letter (FAS), Fluency-Category (Animals)]; visuo-spatial ability [Rey Complex Figure Test and Recognition Trial (RCFT) Copy]; speed of information processing (Trails A and B); symptom validity and functional status [SF-36 Physical Component Score (PCS) and Mental Component Score (MCS)]. We also evaluated the subject's emotional status using Beck Depression Inventory II, Geriatric Depression Scale, and Profile of Mood State Total Mood Disturbance.

Statistical Analysis

Descriptive statistics were calculated for patient demographics and clinical characteristics. Unless otherwise stated, data are expressed as mean ± standard deviation. Subjects were partitioned into three groups according to Clinical Dementia Rating (CDR; 0.5, questionable impairment; 1, mild cognitive impairment; 2, moderate cognitive impairment) (56). The subjects were also partitioned into groups according to the neuropsychometric diagnosis (normal cognition versus impaired cognition).

To produce combined indices of retinal vascular and amyloid measures, each variable was first inspected for normality; any non-normal variables were then log transformed to produce a normal distribution. Each normalized variable was then standardized to a mean of 0 and a standard deviation of 1. While higher amyloid count was associated with worse cognitive function, higher venous vascular tortuosity index (VTI) values were associated with better cognitive function. To account for this inverted scale, the standardized values of venous VTI were multiplied by -1. Standardized variables were then summed to produce exploratory, combined index measures of retinal amyloid and retinal vascular features.

Differences in continuous variables between levels of CDR were assessed through one-way analysis of variance (ANOVA). Differences in continuous variables between diagnostic scores were assessed using Student's t-test. Linear regression was performed to assess the relationship between retinal vascular and retinal amyloid measures, as well as the relationship between combined retinal vascular and amyloid counts and cognitive parameters. All statistical analyses were performed using STATA v15.1 (StataCorp, College Station, TX) with an a priori significance level of 0.05.

Results

Our study included a total of 34 subjects that presented to our Neurology clinic with cognitive concerns. Of those, 29 had retinal images of necessary quality to undergo both retinal amyloid and vascular analysis. Subject demographics and preexisting conditions are shown in Table 1. Mean MOCA was 26 (range 4–32) and median was 27. On formal neuropsychometric cognitive evaluation, 11 (37.93%) patients had normal cognition and 18 (62.06%) had impaired cognition (6 amnestic MCI, 9 multidomain MCI, 2 probable AD and 1 possible fronto-temporal lobar degeneration). Eleven subjects had a CDR of 0.5, 15 had a CDR of 1, and 3 had a CDR of 2.

Linear regression analyses revealed that venous branching angle correlated with distal mid-periphery amyloid count ($p = 0.03$) and arterial inflexion index correlated with posterior pole amyloid count ($p = 0.02$). There were no associations between retinal vascular parameters and amyloid count in the proximal mid-periphery (Supplemental Table 1).

Analysis of retinal vascular and amyloid measures according to strata of cognitive function showed that retinal PMP amyloid count and total amyloid count were significantly higher in the cognitively impaired subjects compared to normal cognition (total: 343 ± 90 versus 247 ± 82, $p = 0.04$; PMP: 144 ± 52 versus 85 ± 32, $p = 0.0012$; Fig. 1D, E). There was no significant difference in venous branching angle ($p = 0.98$) or arterial VTI ($P = 0.53$) across levels of CDR, whereas arterial branching angle reached near significance ($p = 0.066$) (Fig. 1F). Venous VTI was significantly different across levels of CDR (mean ± SD of venous VTI values across increasing CDR categories: 0.13 ± 0.02, 0.13 ± 0.02, 0.09 ± 0.02; $P = 0.026$) (Fig. 1G). Given these group differences, and because of the independence of retinal vascular and retinal amyloid measures, the following combined amyloid-vascular indexes were calculated as exploratory variables: proximal mid-periphery amyloid count-venous VTI, total amyloid count-venous VTI, proximal mid-periphery amyloid count-arterial branching angle, and total amyloid count-arterial branching angle. One-way ANOVA revealed significant group differences in the VTI indices integrated with total retinal or PMP amyloid when compared according to CDR level (Fig. 2A-D). The combined proximal mid-periphery amyloid-venous VTI index exhibited significant group differences when cognitively impaired were compared to cognitively normal subjects (0.49 ± 1.1 versus − 0.91 ± 1.4, $p = 0.006$; Fig. 2E). In this cohort, the combined total retinal amyloid-venous VTI index reached near significance of increased index in the cognitively impaired subjects ($p = 0.09$; Fig. 2F).

We next performed regression analyses to evaluate the correlations between retinal vascular geometric parameters and retinal amyloid counts with cognitive domain Z-scores. We found that venous branching angle correlated with WAIS-IV-digit span Z-score [beta − 0.045 (SE 0.015), $p = 0.08$]. Total amyloid correlated with SF-36-MCS Z-score [Beta − 0.004 (SE 0.002), $P = 0.046$], whereas proximal mid-periphery amyloid count correlated with two verbal memory measures, CVLT-II Long Delay [Beta − 0.009 (SE 0.003), $P = 0.027$] and WMS-IV LM-II [Beta − 0.007 (SE 0.003), $P = 0.028$]. Distal mid-periphery amyloid count correlated with non-verbal memory, RCFT delayed recall [Beta − 0.01 (SE 0.005), $P = 0.04$] and SF-36-MCS [Beta − 0.014 (SE 0.004), $P = 0.004$].

Finally, the combined proximal mid-periphery amyloid-venous VTI index significantly correlated with both verbal memory performance Z-scores [WMS-IV LM-II (Beta − 0.537 (SE 0.138), P = 0.001] and CVLT-II Long Delay [Beta − 0.370 (SE 0.176), P = 0.046], as well as the mental component of the cognitive-related quality-of-life score [SF-36-MCS; Beta − 0.338 (SE 0.153), P = 0.039; Fig. 3C, D]. The combined total amyloid-venous VTI index also correlated with WMS-IV LM-II [Beta − 0.440 (SE 0.132), P = 0.003] and SF-36-MCS [Beta − 0.302 (SE 0.141), P = 0.045; Fig. 3A, B].

Discussion

This exploratory investigation of retinal fluorescence imaging reveals that the combination of retinal amyloid deposits and venous tortuosity index could predict cognitive impairment, and especially verbal memory loss. Further, this study suggests that retinal proximal mid-periphery amyloid count is a comprehensive indicator of AD-related cognitive functioning. In this cohort, we found that retinal vascular features generally did not correlate with retinal amyloid deposition in the proximal mid-periphery but rather with deposits in the distal mid-periphery and posterior pole regions. Overall, by quantitatively assessing two key measures, vascular disease and amyloid burden, we showed the utility of retinal fluorescence imaging as a potential outcome measure in AD clinical trials.

Microvascular damage as a critical initiator of AD pathology is increasingly recognized (5, 9, 57). Vascular dysregulation leading to cerebral amyloid accumulation, and the link between cerebrovascular disease and dementia, are explained by several mechanisms (4, 5, 58). Pericyte loss and deficient vascular platelet-derived growth factor receptor-β signaling were identified in both retinal and cerebral vasculature in subjects with MCI and AD (4, 26). Prior reports demonstrated that retinal vasculature may be used as a biomarker of early or preclinical AD (59), and retinal microvascular abnormalities in AD have been demonstrated using various retinal vasculature imaging modalities (e.g. retinal fundus photography (46, 60, 61), optical coherence tomography angiography (62, 63), high-frequency flicker light stimulation (49, 64), and retinal function imaging (62)). Conversely, den Haan et al (65) showed that retinal vascular measures did not differ between patients with AD and control participants, and venular tortuosity was smaller in subjects with greater white matter disease burden. Tortuosity is a common arteriolar and venular feature found to be associated with vascular disease and aging. We noted a significant difference (p = 0.026) in venous tortuosity between patients with low (0.5) and high (2) CDR, as patients with higher CDR had lower venous tortuosity indices. Our results are in agreement with a prior study (66) that found less tortuous venules in AD patients compared to controls without cognitive decline (p = 0.0244), in a similarly analyzed retinal region that included 0.5-to-2.0 disc diameters away from the optic disc margin. In addition, a study by Williams et al. (67) showed that subjects with lower arteriolar tortuosity were more likely to have AD after appropriate adjustment, whereas no significant variations in venular tortuosity were detected. In contrast to our findings, another study that explored the association between retinal vascular tortuosity and cognitive impairment showed that subjects with increased arteriolar and venular tortuosity were more likely to have AD when compared with cognitively intact controls (60). The disparity in these findings could be explained by the various methods and software

that were used to calculate vessel tortuosity and/or by including different retinal regions of interest in the vascular analysis.

Previous investigations have also shown a strong relationship between retinal vasculopathy and brain amyloid deposition (28), providing compelling evidence for the vascular hypothesis of AD. Sharafi et al. (28) evaluated the relationship between retinal vascular status (vessel diameter, tortuosity and spatial-spectral texture measures) using hyperspectral retinal imaging and CNS amyloid status assessed with (18) F-florbetaben positron-emission tomography. They found that retinal venules of amyloid-positive subjects showed a higher mean tortuosity compared with the amyloid-negative subjects. This pilot study suggested that the inclusion of metrics related to retinal vasculature and surrounding tissue-related texture could improve the discrimination performance of the cerebral amyloid status (28).

As both retinal amyloid accumulation and retinal vascular pathology (26, 32–35) are reported in patients with early or preclinical AD, we explored the interplay between retinal vascular geometric measures and retinal amyloid burden using retinal fluorescence imaging. Prior studies showed that amyloid quantification in the retinal proximal mid-periphery may best reflect cerebral AD pathology, as it correlates with cognitive performance and hippocampal volume (33, 35). In this cohort, we found that retinal vascular features correlate with amyloid deposition in the posterior pole and retinal distal mid-periphery, but not the proximal mid-periphery. A possible explanation is that this investigation measured physical features of the retinal vasculature (e.g., branching angle and tortuosity index), and did not assess functional endpoints. In addition, our quantitative vascular analysis could not target the smaller retinal blood vessels. The mechanisms driving vascular remodeling and amyloid deposition may occur at different rates, leading to the appearance of these clinical signs at different stages in disease progression. The investigation of subjects with mainly mild cognitive impairment in our cohort may explain why venous VTI was lower in subjects with worse cognition, and why the other arterial or venous vascular parameters did not show any significant differences across cognitive strata. This hypothesis is supported by the lack of association between retinal vascular features and most of the neuropsychometric cognitive scores in our cohort. Whereas retinal vascular measures did not correlate with any cognitive measures except for attention and concentration, total and proximal mid-periphery retinal amyloid correlated with verbal memory measures, and distal mid-periphery amyloid count correlated with non-verbal memory. Interestingly, in this cohort with early cognitive disorders, subjects with higher amyloid count and worse cognition had lower retinal venular tortuosity. The only combined index that discriminated between individuals with impaired cognition and normal cognition was proximal mid-periphery amyloid count-venular VTI. This combined index was also associated with verbal memory and the ‘mental component’ summary of psychological functioning (SF-36 Mental Component Score). This later finding reflects the association with the AD-related psychological and emotional functioning. This appears to represent an exclusive contribution, as physical functioning status (SF-36 Physical Component Score) was not associated with amyloid or vascular retinal markers.

In a prior study, two or more retinal vascular abnormalities were associated in a dose-response manner with an increased risk of disabling dementia (47). It is possible that combined amyloid-vascular indexes

are better discriminators of AD, with potential for use as outcome measures in AD trials.

Our findings underscore the potential value of the exploratory amyloid-vascular indexes presented herein. Future investigations are warranted to explore the clinical utility of retinal fluorescence imaging in concert with combined amyloid-vascular index measures. More comprehensive cohort studies including a larger sample size, a greater range of disease severity among the participants, and age-matched controls could help to elucidate the stage at which retinal amyloid and/or retinal venular versus arterial impairments begin to develop, while further developing clinical tools for the detection and characterization of AD. Given the cost and technical requirements of gold-standard methods for assessing cerebral amyloid deposition and vascular pathology, further validation of these retinal imaging methods could potentially yield greater accessibility to testing, thus facilitating more extensive clinical trials as well as improved detection of AD.

Limitations

Our pilot study is limited by a small sample size and heterogeneity. Due to limited numbers, we could not adjust for the presence of traditional vascular risk factors or the presence of retinopathy, which are known contributors to retinal vascular geometric changes. Given the heterogeneity in sample size across study groups and small numbers of probable AD patients, further confirmation of these preliminary findings is needed.

Conclusions

This work reports a pilot retinal imaging-based investigation of the interaction between two reported biomarkers of Alzheimer's disease (AD) – vasculopathy and amyloidopathy – in a small cohort of subjects mostly with mild cognitive impairment. This integrated approach holds the potential advantage of assessing both a hypothesized driver of AD, vascular impairment, as well as the hallmark pathological marker of AD, amyloid deposition. These biomarkers were quantitatively examined in the retina, a central nervous system organ that allows for direct, non-invasive, and high-resolution imaging. We found that the combined amyloid count in the retinal proximal mid-periphery and retinal venular tortuosity correlated with verbal memory and the mental component of the psychological functioning SF-36. Our quantitative assessments of these two key measures may validate retinal fluorescence imaging as a useful outcome parameter in AD clinical trials.

Declarations

Ethical Approval and Consent to participate: This study was approved by the Cedars-Sinai Institutional Review Board under Pro00052349. All participants gave written consent to participate.

Consent for Publication: Not applicable.

Availability of Data and Materials: The datasets used and/or analysed during the current study are available from the corresponding author on reasonable request.

Competing Interests: Black, Verdooner, Koronyo and Koronyo-Hamaoui are founding members of NeuroVision Imaging Inc., 1395 Garden Highway, Suite 250, Sacramento, CA 95833, USA. Dr. Frautschy is co-inventor on US patent US9192644B2 for a curcumin formulation. Johnson, Czeszynski, Verdooner are currently employed by NeuroVision Imaging Inc. The remaining authors declare that the research was conducted in the absence of any commercial or financial relationships that could be construed as a potential conflict of interest.

Funding: We received support from a National Institute on Aging award (AG044897, Koronyo-Hamaoui, PI) and The Saban, The Gordon and The Marciano Private Foundations (Koronyo-Hamaoui, PI). The funders had no role in the design or conduct of this research.

Authors' Contributions:

Research design: OD, RR, AS, DS, KB, PD, SC, YK, MKH; Data acquisition: OD, DS, AS, JS, MKH; Data analysis: RR, DS, JS, TT, KO, AD, SV, KB, YK, PD, YS, SC, MKH; Data interpretation: OD, RR, DS, TT, KB, DTF, YK, PD, SC, ZF, MKH; Manuscript preparation: OD, RR, DTF, SC, YK, MKH.

Acknowledgements: We thank Mia Oviatt for manuscript editing. The authors dedicate the manuscript to the memory of Dr. Salomon Moni Hamaoui and Lillian Jones Black, who died of Alzheimer's disease.

Authors' Information: Not Applicable.

References

1. Hebert LE, Weuve J, Scherr PA, Evans DA. Alzheimer disease in the United States (2010-2050) estimated using the 2010 census. Neurology. 2013;80(19):1778-83.
2. figures Asdfa. Alzheimer's Dement 2020;16:391–460; DOI: 101002/alz12068.
3. Bell RD, Zlokovic BV. Neurovascular mechanisms and blood-brain barrier disorder in Alzheimer's disease. Acta Neuropathol. 2009;118(1):103-13.
4. Montagne A, Nation DA, Sagare AP, Barisano G, Sweeney MD, Chakhoyan A, et al. APOE4 leads to blood-brain barrier dysfunction predicting cognitive decline. Nature. 2020;581(7806):71-6.
5. He JT, Zhao X, Xu L, Mao CY. Vascular Risk Factors and Alzheimer's Disease: Blood-Brain Barrier Disruption, Metabolic Syndromes, and Molecular Links. J Alzheimers Dis. 2020;73(1):39-58.
6. Riphagen JM, Ramakers I, Freeze WM, Pagen LHG, Hanseeuw BJ, Verbeek MM, et al. Linking APOE-epsilon4, blood-brain barrier dysfunction, and inflammation to Alzheimer's pathology. Neurobiol Aging. 2020;85:96-103.
7. Nikolakopoulou AM, Montagne A, Kisler K, Dai Z, Wang Y, Huuskonen MT, et al. Pericyte loss leads to circulatory failure and pleiotrophin depletion causing neuron loss. Nat Neurosci. 2019;22(7):1089-98.

8. Solis E, Hascup KN, Hascup ER. Alzheimer's Disease: The Link Between Amyloid-beta and Neurovascular Dysfunction. J Alzheimers Dis. 2020;76(4):1179-98.
9. Sweeney MD, Montagne A, Sagare AP, Nation DA, Schneider LS, Chui HC, et al. Vascular dysfunction-The disregarded partner of Alzheimer's disease. Alzheimers Dement. 2019;15(1):158-67.
10. Quinones AR, Kaye J, Allore HG, Botoseneanu A, Thielke SM. An Agenda for Addressing Multimorbidity and Racial and Ethnic Disparities in Alzheimer's Disease and Related Dementia. Am J Alzheimers Dis Other Demen. 2020;35:1533317520960874.
11. Jack CR, Jr., Bennett DA, Blennow K, Carrillo MC, Dunn B, Haeberlein SB, et al. NIA-AA Research Framework: Toward a biological definition of Alzheimer's disease. Alzheimers Dement. 2018;14(4):535-62.
12. Mantzavinos V, Alexiou A. Biomarkers for Alzheimer's Disease Diagnosis. Curr Alzheimer Res. 2017;14(11):1149-54.
13. Olsson B, Lautner R, Andreasson U, Ohrfelt A, Portelius E, Bjerke M, et al. CSF and blood biomarkers for the diagnosis of Alzheimer's disease: a systematic review and meta-analysis. Lancet Neurol. 2016;15(7):673-84.
14. Allegri RF, Chrem Mendez P, Calandri I, Cohen G, Martin ME, Russo MJ, et al. Prognostic value of ATN Alzheimer biomarkers: 60-month follow-up results from the Argentine Alzheimer's Disease Neuroimaging Initiative. Alzheimers Dement (Amst). 2020;12(1):e12026.
15. Baldacci F, Mazzucchi S, Della Vecchia A, Giampietri L, Giannini N, Koronyo-Hamaoui M, et al. The path to biomarker-based diagnostic criteria for the spectrum of neurodegenerative diseases. Expert Rev Mol Diagn. 2020;20(4):421-41.
16. Sweeney MD, Sagare AP, Zlokovic BV. Blood-brain barrier breakdown in Alzheimer disease and other neurodegenerative disorders. Nat Rev Neurol. 2018;14(3):133-50.
17. Kisler K, Nelson AR, Montagne A, Zlokovic BV. Cerebral blood flow regulation and neurovascular dysfunction in Alzheimer disease. Nat Rev Neurosci. 2017;18(7):419-34.
18. Shi H, Koronyo Y, Fuchs DT, Sheyn J, Wawrowsky K, Lahiri S, et al. Retinal capillary degeneration and blood-retinal barrier disruption in murine models of Alzheimer's disease. Acta Neuropathol Commun. 2020;8(1):202.
19. Hart NJ, Koronyo Y, Black KL, Koronyo-Hamaoui M. Ocular indicators of Alzheimer's: exploring disease in the retina. Acta Neuropathol. 2016;132(6):767-87.
20. Koronyo-Hamaoui M, Koronyo Y, Ljubimov AV, Miller CA, Ko MK, Black KL, et al. Identification of amyloid plaques in retinas from Alzheimer's patients and noninvasive in vivo optical imaging of retinal plaques in a mouse model. Neuroimage. 2011;54 Suppl 1:S204-17.
21. Koronyo Y, Salumbides BC, Black KL, Koronyo-Hamaoui M. Alzheimer's disease in the retina: imaging retinal abeta plaques for early diagnosis and therapy assessment. Neurodegener Dis. 2012;10(1-4):285-93.
22. Tsai Y, Lu B, Ljubimov AV, Girman S, Ross-Cisneros FN, Sadun AA, et al. Ocular changes in TgF344-AD rat model of Alzheimer's disease. Invest Ophthalmol Vis Sci. 2014;55(1):523-34.

23. La Morgia C, Ross-Cisneros FN, Koronyo Y, Hannibal J, Gallassi R, Cantalupo G, et al. Melanopsin retinal ganglion cell loss in Alzheimer disease. Ann Neurol. 2016;79(1):90-109.
24. den Haan J, Morrema THJ, Verbraak FD, de Boer JF, Scheltens P, Rozemuller AJ, et al. Amyloid-beta and phosphorylated tau in post-mortem Alzheimer's disease retinas. Acta Neuropathol Commun. 2018;6(1):147.
25. Grimaldi A, Pediconi N, Oieni F, Pizzarelli R, Rosito M, Giubettini M, et al. Neuroinflammatory Processes, A1 Astrocyte Activation and Protein Aggregation in the Retina of Alzheimer's Disease Patients, Possible Biomarkers for Early Diagnosis. Front Neurosci. 2019;13:925.
26. Shi H, Koronyo Y, Rentsendorj A, Regis GC, Sheyn J, Fuchs DT, et al. Identification of early pericyte loss and vascular amyloidosis in Alzheimer's disease retina. Acta Neuropathol. 2020;139(5):813-36.
27. Habiba U, Merlin S, Lim JKH, Wong VHY, Nguyen CTO, Morley JW, et al. Age-Specific Retinal and Cerebral Immunodetection of Amyloid-beta Plaques and Oligomers in a Rodent Model of Alzheimer's Disease. J Alzheimers Dis. 2020;76(3):1135-50.
28. Sharafi SM, Sylvestre JP, Chevrefils C, Soucy JP, Beaulieu S, Pascoal TA, et al. Vascular retinal biomarkers improves the detection of the likely cerebral amyloid status from hyperspectral retinal images. Alzheimers Dement (N Y). 2019;5:610-7.
29. Vit JP, Fuchs DT, Angel A, Levy A, Lamensdorf I, Black KL, et al. Color and contrast vision in mouse models of aging and Alzheimer's disease using a novel visual-stimuli four-arm maze. Sci Rep. 2021;11(1):1255.
30. Mirzaei N, Shi H, Oviatt M, Doustar J, Rentsendorj A, Fuchs DT, et al. Alzheimer's Retinopathy: Seeing Disease in the Eyes. Front Neurosci. 2020;14:921.
31. Snyder PJ, Alber J, Alt C, Bain LJ, Bouma BE, Bouwman FH, et al. Retinal imaging in Alzheimer's and neurodegenerative diseases. Alzheimers Dement. 2021;17(1):103-11.
32. Koronyo Y, Biggs D, Barron E, Boyer DS, Pearlman JA, Au WJ, et al. Retinal amyloid pathology and proof-of-concept imaging trial in Alzheimer's disease. JCI Insight. 2017;2(16).
33. Dumitrascu OM LP, Torbati T, et al. Sectoral segmentation of retinal amyloid imaging in subjects with cognitive decline. Alzheimer’s Dement. 2020;e12109. https://doi.org/10.1002/dad2.12109.
34. Schultz N, Byman E, Netherlands Brain B, Wennstrom M. Levels of Retinal Amyloid-beta Correlate with Levels of Retinal IAPP and Hippocampal Amyloid-beta in Neuropathologically Evaluated Individuals. J Alzheimers Dis. 2020;73(3):1201-9.
35. Lee S, Jiang K, McIlmoyle B, To E, Xu QA, Hirsch-Reinshagen V, et al. Amyloid Beta Immunoreactivity in the Retinal Ganglion Cell Layer of the Alzheimer's Eye. Front Neurosci. 2020;14:758.
36. Doustar J, Torbati T, Black KL, Koronyo Y, Koronyo-Hamaoui M. Optical Coherence Tomography in Alzheimer's Disease and Other Neurodegenerative Diseases. Front Neurol. 2017;8:701.
37. Hampel H, Toschi N, Babiloni C, Baldacci F, Black KL, Bokde ALW, et al. Revolution of Alzheimer Precision Neurology. Passageway of Systems Biology and Neurophysiology. J Alzheimers Dis. 2018;64(s1):S47-S105.

38. Carare RO, Aldea R, Agarwal N, Bacskai BJ, Bechman I, Boche D, et al. Clearance of interstitial fluid (ISF) and CSF (CLIC) group-part of Vascular Professional Interest Area (PIA): Cerebrovascular disease and the failure of elimination of Amyloid-beta from the brain and retina with age and Alzheimer's disease-Opportunities for Therapy. Alzheimers Dement (Amst). 2020;12(1):e12053.
39. N M. Shi H, Oviatt M. et al. Alzheimer’s Retinopathy: Seeing Disease in The Eyes. Front Neurosci . 14:921 (2020). doi: 10.3389/fnins.2020.00921. 2020.
40. Cabrera DeBuc D, Somfai GM, Arthur E, Kostic M, Oropesa S, Mendoza Santiesteban C. Investigating Multimodal Diagnostic Eye Biomarkers of Cognitive Impairment by Measuring Vascular and Neurogenic Changes in the Retina. Front Physiol. 2018;9:1721.
41. Uemura MT, Maki T, Ihara M, Lee VMY, Trojanowski JQ. Brain Microvascular Pericytes in Vascular Cognitive Impairment and Dementia. Front Aging Neurosci. 2020;12:80.
42. McGrory S, Cameron JR, Pellegrini E, Warren C, Doubal FN, Deary IJ, et al. The application of retinal fundus camera imaging in dementia: A systematic review. Alzheimers Dement (Amst). 2017;6:91-107.
43. Deal JA, Sharrett AR, Rawlings AM, Gottesman RF, Bandeen-Roche K, Albert M, et al. Retinal signs and 20-year cognitive decline in the Atherosclerosis Risk in Communities Study. Neurology. 2018;90(13):e1158-e66.
44. Deal JA, Sharrett AR, Albert M, Bandeen-Roche K, Burgard S, Thomas SD, et al. Retinal signs and risk of incident dementia in the Atherosclerosis Risk in Communities study. Alzheimers Dement. 2019;15(3):477-86.
45. Jung NY, Han JC, Ong YT, Cheung CY, Chen CP, Wong TY, et al. Retinal microvasculature changes in amyloid-negative subcortical vascular cognitive impairment compared to amyloid-positive Alzheimer's disease. J Neurol Sci. 2019;396:94-101.
46. Frost S, Bhuiyan A, Offerman D, Doecke JD, Macaulay SL, Sohrabi HR, et al. Modulation of Retinal Arteriolar Central Reflection by APOE Genotype. Curr Alzheimer Res. 2017;14(9):916-23.
47. Jinnouchi H, Kitamura A, Yamagishi K, Kiyama M, Imano H, Okada T, et al. Retinal Vascular Changes and Prospective Risk of Disabling Dementia: the Circulatory Risk in Communities Study (CIRCS). J Atheroscler Thromb. 2017;24(7):687-95.
48. Dumitrascu OM, Demaerschalk BM, Valencia Sanchez C, Almader-Douglas D, O'Carroll CB, Aguilar MI, et al. Retinal Microvascular Abnormalities as Surrogate Markers of Cerebrovascular Ischemic Disease: A Meta-Analysis. J Stroke Cerebrovasc Dis. 2018;27(7):1960-8.
49. Golzan SM, Goozee K, Georgevsky D, Avolio A, Chatterjee P, Shen K, et al. Retinal vascular and structural changes are associated with amyloid burden in the elderly: ophthalmic biomarkers of preclinical Alzheimer's disease. Alzheimers Res Ther. 2017;9(1):13.
50. Kobe T, Gonneaud J, Pichet Binette A, Meyer PF, McSweeney M, Rosa-Neto P, et al. Association of Vascular Risk Factors With beta-Amyloid Peptide and Tau Burdens in Cognitively Unimpaired Individuals and Its Interaction With Vascular Medication Use. JAMA Netw Open. 2020;3(2):e1920780.

51. Khansari MM, Garvey SL, Farzad S, Shi Y, Shahidi M. Relationship between retinal vessel tortuosity and oxygenation in sickle cell retinopathy. Int J Retina Vitreous. 2019;5:47.
52. Frangi FA NW, Vincken KL, Viergever MA. Multiscale vessel enhancement filtering1998. 130–7 p.
53. Ayub L KA, Ayub J, Ayub S, Akram S, Irshad S, "Differentiation of blood vessels in retina into arteries and veins using neural network," 2016 International Conference on Computing, Electronic and Electrical Engineering (ICE Cube), Quetta. 2016:301-6.
54. Khansari MM, O'Neill W, Lim J, Shahidi M. Method for quantitative assessment of retinal vessel tortuosity in optical coherence tomography angiography applied to sickle cell retinopathy. Biomed Opt Express. 2017;8(8):3796-806.
55. Bullitt E, Gerig G, Pizer SM, Lin W, Aylward SR. Measuring tortuosity of the intracerebral vasculature from MRA images. IEEE Trans Med Imaging. 2003;22(9):1163-71.
56. Morris JC. The Clinical Dementia Rating (CDR): current version and scoring rules. Neurology. 1993;43(11):2412-4.
57. Nation DA, Sweeney MD, Montagne A, Sagare AP, D'Orazio LM, Pachicano M, et al. Blood-brain barrier breakdown is an early biomarker of human cognitive dysfunction. Nat Med. 2019;25(2):270-6.
58. Goulay R, Mena Romo L, Hol EM, Dijkhuizen RM. From Stroke to Dementia: a Comprehensive Review Exposing Tight Interactions Between Stroke and Amyloid-beta Formation. Transl Stroke Res. 2020;11(4):601-14.
59. O'Bryhim BE, Apte RS, Kung N, Coble D, Van Stavern GP. Association of Preclinical Alzheimer Disease With Optical Coherence Tomographic Angiography Findings. JAMA Ophthalmol. 2018;136(11):1242-8.
60. Cheung CY, Ong YT, Ikram MK, Ong SY, Li X, Hilal S, et al. Microvascular network alterations in the retina of patients with Alzheimer's disease. Alzheimers Dement. 2014;10(2):135-42.
61. Csincsik L, MacGillivray TJ, Flynn E, Pellegrini E, Papanastasiou G, Barzegar-Befroei N, et al. Peripheral Retinal Imaging Biomarkers for Alzheimer's Disease: A Pilot Study. Ophthalmic Res. 2018;59(4):182-92.
62. Jiang H, Liu Y, Wei Y, Shi Y, Wright CB, Sun X, et al. Impaired retinal microcirculation in patients with Alzheimer's disease. PLoS One. 2018;13(2):e0192154.
63. van de Kreeke JA, Nguyen HT, Konijnenberg E, Tomassen J, den Braber A, Ten Kate M, et al. Optical coherence tomography angiography in preclinical Alzheimer's disease. Br J Ophthalmol. 2020;104(2):157-61.
64. Bettermann K, Slocomb JE, Shivkumar V, Lott ME. Retinal vasoreactivity as a marker for chronic ischemic white matter disease? J Neurol Sci. 2012;322(1-2):206-10.
65. den Haan J, van de Kreeke JA, van Berckel BN, Barkhof F, Teunissen CE, Scheltens P, et al. Is retinal vasculature a biomarker in amyloid proven Alzheimer's disease? Alzheimers Dement (Amst). 2019;11:383-91.

66. Frost S, Kanagasingam Y, Sohrabi H, Vignarajan J, Bourgeat P, Salvado O, et al. Retinal vascular biomarkers for early detection and monitoring of Alzheimer's disease. Transl Psychiatry. 2013;3:e233.
67. Williams MA, McGowan AJ, Cardwell CR, Cheung CY, Craig D, Passmore P, et al. Retinal microvascular network attenuation in Alzheimer's disease. Alzheimers Dement (Amst). 2015;1(2):229-35.

Tables

Table 1. Demographics and Medical History of subjects in the combined retinal vascular and retinal amyloid analysis	
N (% Female)	29 (55)
Age (years)	64 ± 6
Preexisting Health Conditions, N (%)	
Hypertension	11 (38)
Hyperlipidemia	15 (52)
Diabetes	3 (10)
Hyperthyroidism	8 (28)
Stroke/TIA	1 (3)
Heart Disease/CAD/CHF	1 (3)
Smoking h/o	2 (7)

Supplementary Tables

Supplemental Table 1 is not available with this version.

Figures

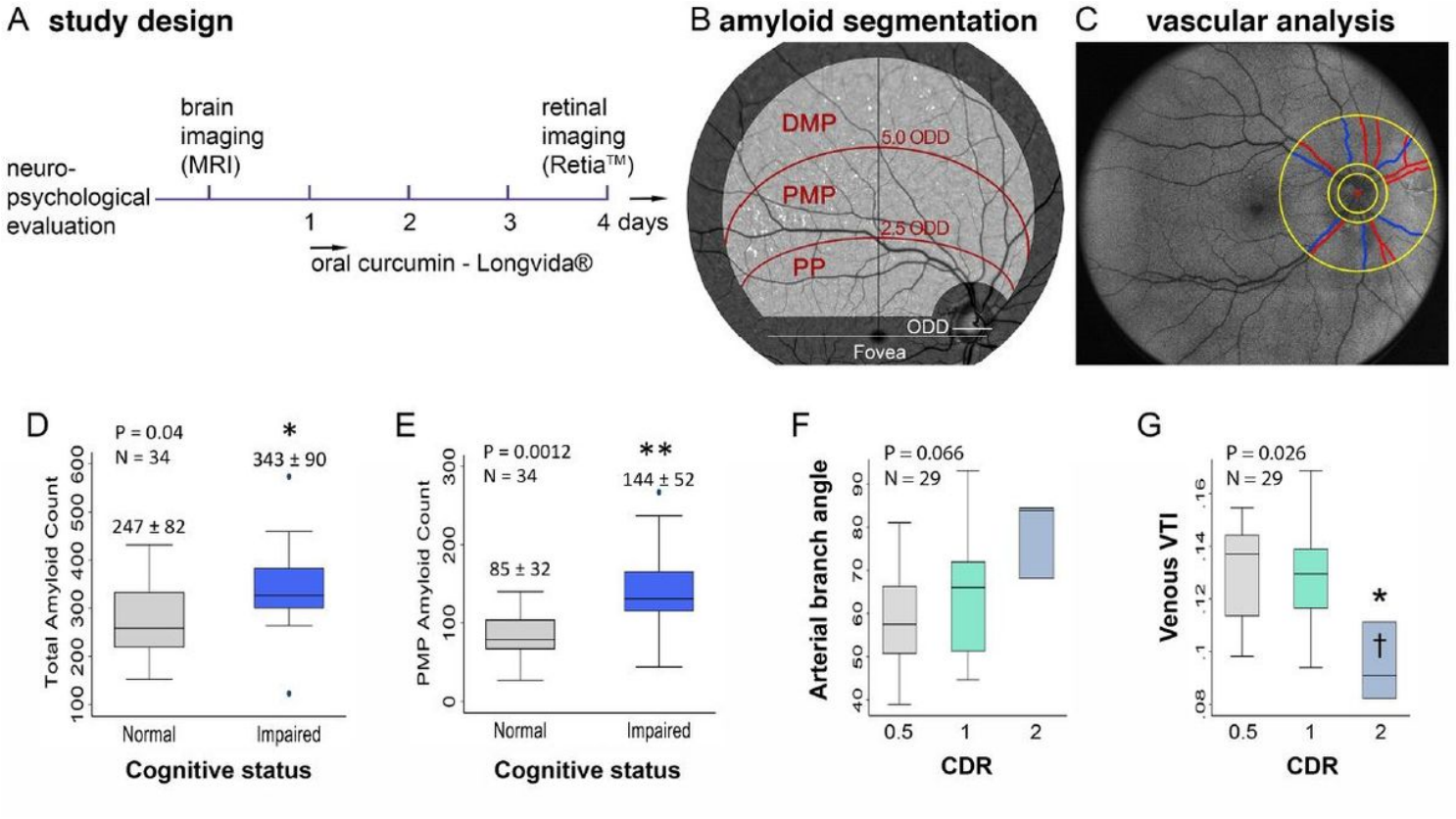

Figure 1

Study timeline of brain and retinal imaging followed by sectoral amyloid and vascular analysis. Study design scheme illustrating that subject underwent baseline brain imaging and neuropsycological evaluation, followed by retinal fluorescence imaging after 4 days of daily oral curcumin intake (A). Illustration of the region of interest in the right eye supero-temporal retinal quadrant and its three subregions, which were used for quantifying retinal amyloid counts (B). Illustration of the region of interest used for the retinal vascular analysis. The red circle indicates the center of optic nerve head and the smallest yellow circle shows optic nerve head area. The two larger circles demonstrate the region of interest for vascular analysis which are 1.5- and 4-times the diameter of the optic disc. The branching angle and tortuosity of vessels within the region of interest were calculated. Arteries and veins are outlined by red and blue lines, respectively (C). Graphs illustrating differences in total amyloid (D) and proximal amyloid counts (E) when stratified by cognitive status. Graphs illustrating the differences between arterial branching angle (F) and venous tortuosity index (G) when stratified by CDR. Abbreviations: MRI, magnetic resonance imaging; PP, posterior pole; PMP, proximal mid-periphery; DMP, distal mid-periphery; ODD, optic disc diameter; CDR, Clinical Dementia Rating; VTI, vessel tortuosity index

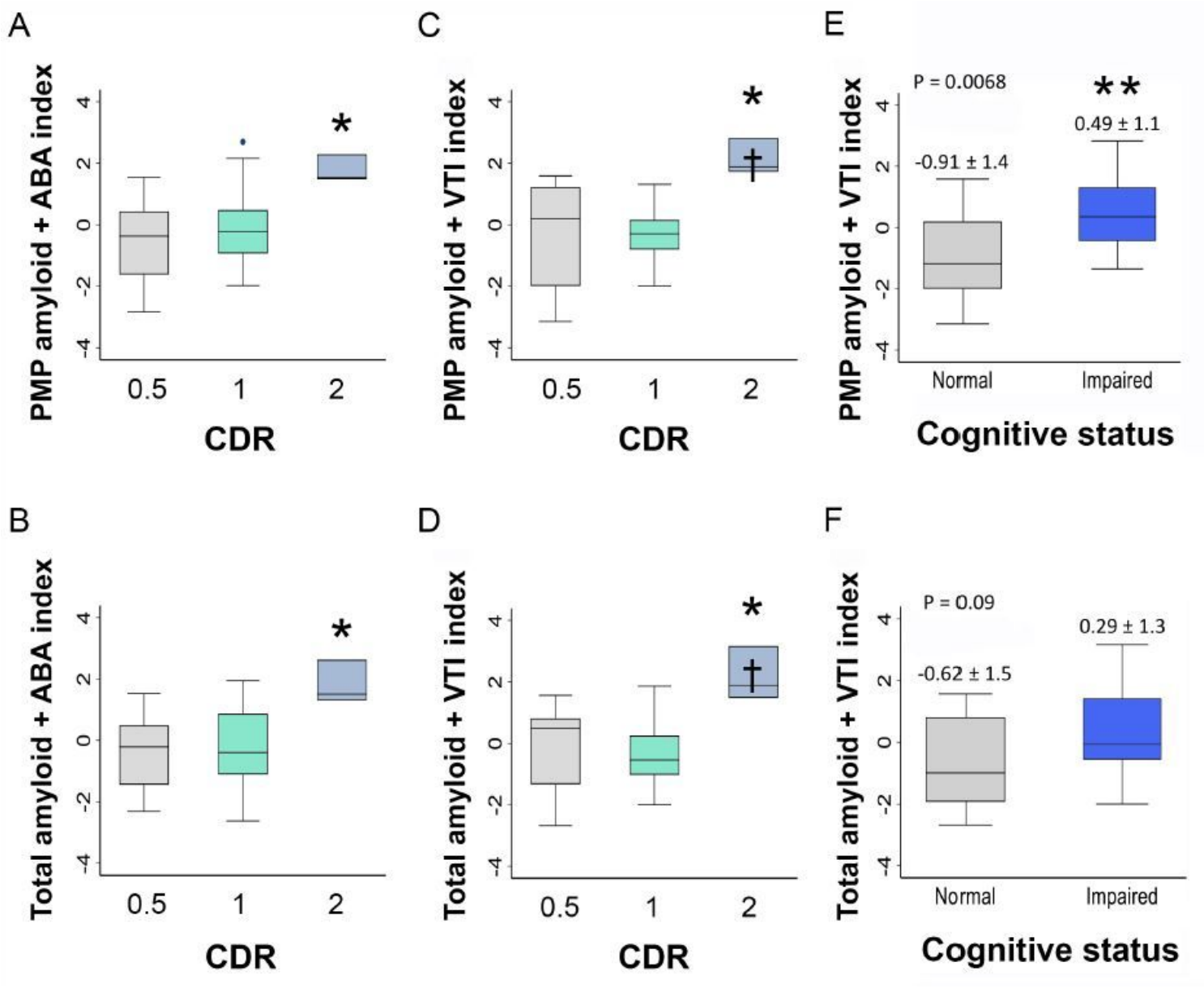

Figure 2

Combined retinal amyloid and vascular parameters in patients stratified by cognitive scores. Graphs illustrating the differences in the combined proximal mid-periphery amyloid - arterial branching angle index (A), total amyloid - arterial branching angle index (B), proximal mid-periphery amyloid - venous tortuosity index (C) and total amyloid - venous tortuosity index (D) when stratified by CDR score. Graphs illustrating the differences between the combined proximal mid periphery amyloid - venous tortuosity index (E) and total amyloid- venous tortuosity index (F) when stratified by the cognitive status. Bar graphs are showing mean and deviation (* P < .05, ** P < .01 by two-tailed paired Student t test). Abbreviations: VTI, vessel tortuosity index; ABA, arterial branching angle; PMP, proximal mid-periphery; CDR, Clinical Dementia Rating.

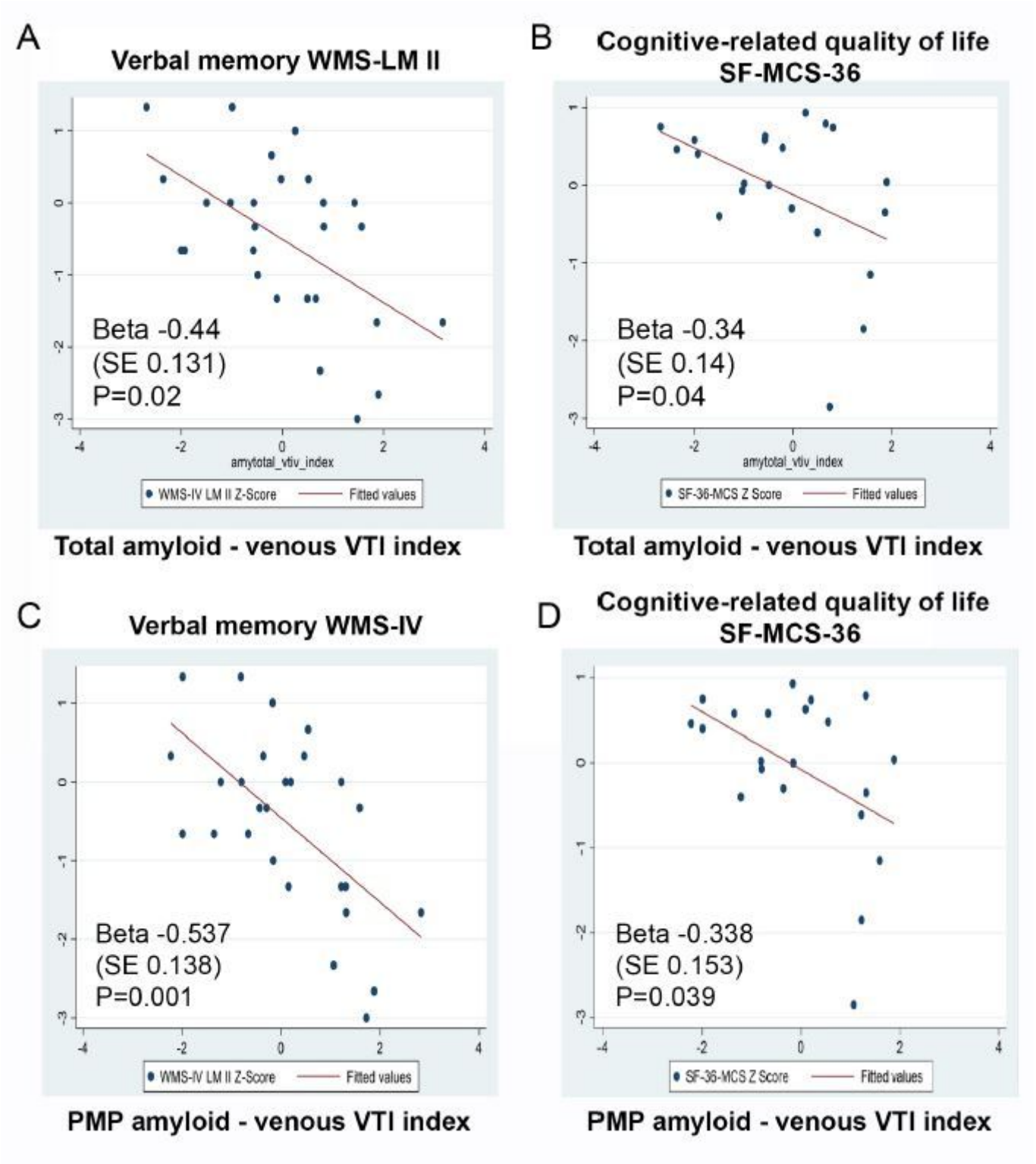

Figure 3

Retinal amyloid count combined with retinal venous VTI correlates with verbal memory and cognitive-related quality of life measures. Graphs illustrating the correlations between the combined total amyloid - venous tortuosity index and verbal memory (A) and cognitive-related quality of life Z-scores (B), and the correlations between the combined proximal mid-periphery amyloid-venous tortuosity index and verbal memory (C) and cognitive-related quality of life Z-scores (D). Abbreviations: WMS-IV LM II, Wechsler

Memory Scale IV Logical Memory II; WMS-IV, Wechsler Memory Scale IV; SF-36 MCS, SF-36 Mental Component Score; PMP, proximal mid-periphery; VTI, vessel tortuosity index.